

Original Paper

# ASMase is Essential for the Immune Response to Partial-Tumor Radiation Exposure

Mickael Mathieu<sup>a,b</sup> Prerna R. Nepali<sup>b</sup> James Russell<sup>c</sup> Hadi Askarifirouzjaei<sup>b</sup>  
Melis Baltaci<sup>b</sup> Simon N. Powell<sup>b</sup> John Humm<sup>c</sup> Joseph O. Deasy<sup>c</sup>  
Adriana Haimovitz-Friedman<sup>b\*</sup>

<sup>a</sup>Clinical Research Unit, Emile Roux Hospital Center, Le Puy-en-Velay, France, <sup>b</sup>Department of Radiation Oncology, Memorial Sloan Kettering Cancer Center, New York City, NY, USA, <sup>c</sup>Department of Medical Physics, Memorial Sloan Kettering Cancer Center, New York City, NY, USA

## Key Words

Acid Sphingomyelinase • Partial Volume Radiotherapy • Immune Response • STING

## Abstract

**Background/Aims:** Tumor response to radiation is thought to depend on the direct killing of tumor cells. Our laboratory has called this into question. Firstly, we showed that the biology of the host, specifically the endothelial expression of acid sphingomyelinase (ASMase), was critical in determining tumor radiocurability. Secondly, we have shown that the immune system can enhance radiation response by allowing a complete tumor control in hemi-irradiated tumors. In this paper, we focus on the integration of these two findings. **Methods:** We used Lewis Lung Carcinoma (LLC) cells, injected in the flank of either: (i) ASMase knockout or (ii) WT of matched background (sv129xBl/6) or (iii) C57Bl/6 mice. Radiation therapy (RT) was delivered to 50% or 100% of the LLC tumor volume. Tumor response, immune infiltration (CD8<sup>+</sup> T cells), ICAM-1, and STING activation were measured. Radiotherapy was also combined with methyl-cyclodextrin, to inhibit the ASMase-mediated formation of ceramide-enriched lipid rafts. **Results:** We recapitulated our previous finding, namely that tumor hemi-irradiation was sufficient for tumor control in the LLC/C57Bl/6 model. However, in ASMase KO mice hemi-irradiation was ineffective. Likewise, pharmacological inhibition of ASMase significantly reduced the tumor response to hemi-irradiation. Further, we demonstrated elevated ICAM-1 expression, increased levels of CD8<sup>+</sup> T cells, ICAM-1, and STING activation in tumors growing in C57Bl/6 mice, as well as the ASMase WT strain. However, no such changes were seen in tumors growing in ASMase KO mice. **Conclusion:** ASMase and ceramide generation are necessary to mediate a radiation-induced anti-tumor immune response *via* STING activation.

© 2024 The Author(s). Published by  
Cell Physiol Biochem Press GmbH&Co. KG

## Introduction

Radiation therapy (RT) is commonly used to treat cancer [1]. Initially, it was assumed that RT acted only through cytotoxic effects on the tumor cell population, mediated either by direct unreparable physical DNA damage or indirect damage from reactive oxygen species [2]. However, recent results show that RT also impacts both the tumor microenvironment [3] and tumor immunogenicity, in ways that can significantly affect outcome. Thus, irradiated tumor cells may generate specific molecular signals that trigger an immune response [4-6]. RT can also trigger anti-tumoral responses occurring at a distance from the treatment area. This phenomenon, known as the abscopal effect, has occasionally been reported in the clinic [7, 8], and might also have been observed in patients treated with RT combined with immune checkpoint blockade treatments [9]. The future of RT resides in the modulation of the immune responses involved in tumor control while preserving the normal tissues surrounding the tumors. To achieve this goal, it is imperative to better understand the mechanisms involved in RT-induced immune responses.

If radiation is considered as a direct tumor cell killing agent, it is critical to achieve a uniform dose distribution throughout the tumor volume if tumor cure is to be accomplished. Any untreated volume will harbor surviving clonogens that can repopulate the tumor and cause treatment failure. However, if radiation acts through micro-environmental or immune mechanisms, this consideration no longer necessarily applies. Recently, some clinics have experimented with spatially-fractionated irradiation (SFRT) such as GRID/Lattice RT, which delivers high-dose radiation to small volumes within a tumor target [10, 11], and has been linked to bystander effects [12], but also potentially aided by activation of the host immune system [1].

In previous pre-clinical work [13], we explored a very different spatial dose distribution, where murine tumors were given a dose to only half of the tumor volume. Partial volume radiotherapy (PVRT) was successful in controlling tumor growth, even though the radiation exposure could not have directly targeted more than 50% of the tumor cells. In this treatment, very few unirradiated cells would have irradiated neighbors, and so we can discount any bystander effect. Instead, multiple lines of evidence conclusively showed an immune contribution to tumor response. Further, Markovskiy et al. 2018 showed that PVRT induces an increased expression of intracellular adhesion molecule-1 (ICAM-1), which is responsible for lymphocyte recruitment, followed by a significant infiltration of cytotoxic CD8<sup>+</sup> T cells into the tumors [13]. We subsequently found that this response is activated by cGAS/STING [14]. Similar to viral infection, RT induces DNA damage accumulation within the cytoplasm that activates cGAS/STING [15-22], and we demonstrated that PVRT induces an antitumor response by activating STING, which stimulates a specific cytokine signature as part of the immune response. STING activation occurred either via the canonical cGAS/STING pathway or a non-canonical ATM-driven pathway, depending on the tumor model [14].

Earlier work from the laboratory of Fuks and Kolesnick suggests a further route by which RT might produce a therapeutic response, independently of tumor cell kill [23]. Endothelial cells are prone to radiation-induced apoptosis, and this is induced, not by the p53 pathway, but through the activation of acid sphingomyelinase (ASMase), which generates ceramide with changes in membrane structure and the formation of ceramide enriched platforms (CRMs) as an initial step to apoptosis [23-27]. Endothelial cell apoptosis could be reliably induced in tumors by doses over 15Gy, but this effect was absent when ASMase knockout mice were used as the tumor host. Importantly, the radiation response of tumors in the ASMase knockout mice was also significantly attenuated suggesting, but not proving a causal link between endothelial cell apoptosis and tumor radioresponse [23].

Because ceramide has also been linked to immune response, we investigated the role of ASMase after PVRT. We used a genetic approach first and used the poorly immunogenic and radioresistant Lewis lung carcinoma cells (LLC) model, grown in either wild-type or ASMase KO mice. In addition, we also used a biochemical approach by inhibiting the formation of ceramide-enriched platforms with methyl-cyclodextrin and showed with both approaches

that the sensitivity of LLC tumors to PVRT was ASMase-ceramide dependent. Furthermore, all the associated upstream events: STING activation, ICAM-1 upregulation, and tumor infiltration by CD8<sup>+</sup> T cells also required host ASMase-ceramide.

## Materials and Methods

### *Cell culture*

Lewis lung carcinoma cells (from ATCC) were cultured in Dulbecco's modified Eagle's medium (DMEM) supplemented with 10% fetal bovine serum, 2 mM L-glutamine, 100 U/mL penicillin, 100 µg/mL streptomycin and 0.25 µg/mL amphotericin B. Cells were kept in a humidified incubator at 37°C, in 5% CO<sub>2</sub>.

### *Tumor inoculation*

C<sub>57</sub>Bl/6 mice were purchased from Jackson Laboratory (Bar Harbor, ME). ASMase KO and WT were generously provided by Drs. Edward Schuchman (Mount Sinai Medical Center) and Richard Kolesnick (Memorial Sloan Kettering Cancer Center) and bred at the Research Animal Resource Center (RARC) of Memorial Sloan Kettering Cancer Center. By mating ASMase<sup>±</sup> mice, we obtained both ASMase KO (ASMase<sup>-/-</sup>) and WT (+/- and +/+) littermates. Mice were then used at 12 weeks of age, to allow the immune system to mature. LLC cells were injected subcutaneously (s.c.) in the flank. 1.5 × 10<sup>6</sup> cells were injected with 50% Matrigel (Growth Factor Reduced) in PBS. Previous data showed no difference between sexes in our experiments [14]. Therefore, we used both male and female mice in our experiments.

### *Drug injections*

Mice were treated with water (control group) or Methyl-cyclodextrin (100mg/kg, 2h pre-RT & once a week, i.p.) (MCD group) and with an IgG2a antibody (control group) or Ly6G antibody (PMN-depleted group) (200µg/mouse, 24h pre-RT & twice a week, i.p.).

### *Irradiation procedure*

Tumors (mean volume between 150 and 250 mm<sup>3</sup>) were irradiated with either 100% or 50% volume coverage using an XRAD 225C (Precision X-Ray, North Branford CT), with a 2 × 2 cm collimator, at 225kV, 13mA, dose rate of approximately 3.5Gy/min (Supp Fig. 1). The irradiation field was defined using GAF chromic film, and the mouse was positioned so that either all or half of the tumor was in the field. The part of the tumor that was outside of the irradiation field (Off Field=OF) received a dose of <5% of the primary In-Field (IF) dose [13]. OF doses were based on densitometry profiles of radiochromic films, exposed in water phantoms. These were incorporated into an in-house treatment planning system (Metropolis) that was used to create sample plans on CT scans of treated mice. Full details have been published by Jeong et al. [28]. Our initial report [13] contains biologic support for the OF dosimetry. LLC inoculated mice received a single dose of 15Gy. After irradiation, mice were either observed for tumor response or euthanized at 24 hours post-RT to collect the tumor.

### *Immunohistochemistry (IHC) staining*

Staining was performed by the Memorial Sloan Kettering Cancer Center Molecular Cytology Core Facility using a Discovery XT processor (Ventana Medical Systems). Tumors were fixed with 10% formalin, embedded in paraffin, and sectioned at 5µm thickness. Tumors that were 50% irradiated were cut with a scalpel along the edge of the irradiation field (marked on the skin of the mouse) before excision of the tumor and the irradiated and non-irradiated halves were processed separately.

Tissue sections were deparaffinized with EZPrep buffer followed by heat-induced epitope retrieval in a pH 6.0 buffer. Sections were blocked for 30 minutes with Background Buster solution (Innovex). Sections were incubated with primary antibodies (anti-STING antibody: Abcam (ab189430), anti-ICAM-1: R&D Systems (AF796), anti-CD8: Cedarlane (HS-36100(Sy)), and anti-Ly6G: Abcam (ab238132) followed by 60 minutes incubation with the appropriate biotinylated secondary antibody (goat anti-rabbit IgG (Vector labs), goat anti-mouse IgG (Vector labs), and goat anti-rat IgG (Vector labs)). All stains were performed in a Leica Bond RX automated stainer using the Bond Polymer Refine detection system (Leica Biosystem DS9800). The chromogen used was 3, 3 diaminobenzidine tetrachloride and sections were counterstained with hematoxylin.

*Imaging and analysis*

Slides were imaged on a Panoramic 250 slide scanner (3DHISTECH) at 20x resolution. Entire tissue sections were used for analysis. Threshold was adjusted to exclude background and stained regions were quantified using ImageJ.

*Statistical analysis*

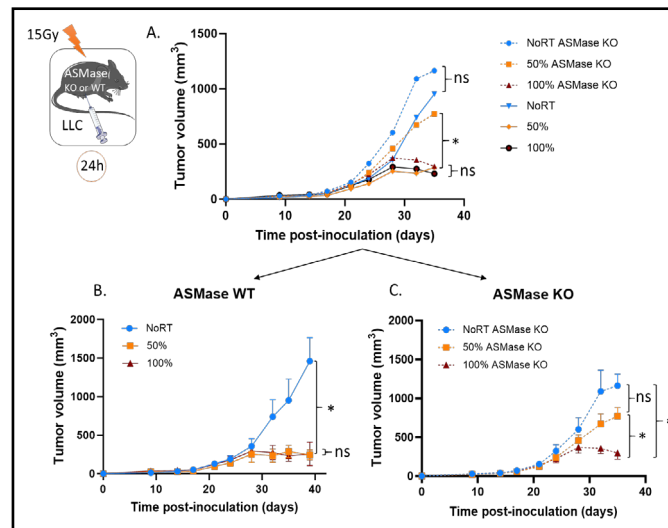
Data are expressed as mean ± SEM. Statistical analyses were performed using 1-way analysis of variance and post hoc Tukey's Multiple comparisons tests or Student's t-test with Welch's correction (Prism 9.0.0; GraphPad). Significance was set at  $P < 0.05$ . The comparisons between all the different groups have been made for each experiment. However, the comparisons that are not of interest are not shown to not overcharge the graphs.

**Results**

*ASMase-ceramide is essential for the PVRT-induced tumor response*

Tumors were irradiated (when mean tumor volume was between 150-250 mm<sup>3</sup>) with a dose of 15Gy using either PVRT or 100% tumor volume exposure in both ASMase KO (ASMase -/-) and ASMase Wild-Type (ASMase +/- or +/+) littermate mice. On the conventional assumption that tumor response to radiation is determined by the extent of tumor cell kill, hemi-irradiation or PVRT, could never affect more than a 50% reduction in viable cell numbers, and hence never induce a growth delay greater than one tumor volume doubling time. In the results reported here, as well as in our lab's previously published paper [13, 14], LLC tumors' response differs markedly from this expectation, with the PVRT tumors being controlled compared to the non-irradiated ones to the same extent as fully irradiated tumors (Fig. 1A-B). There is no effect of the ASMase depletion on the tumor growth without RT. However, when tumors were grown in ASMase KO mice, PVRT became ineffective, as illustrated in Fig. 1A-C. We observed indeed a significant difference between the 50%-irradiated WT and KO groups, as well as a significant difference between the 50% and 100% tumors in the ASMase KO mice, demonstrating the essential role of ASMase in the PVRT-induced tumor response. There was no difference between the tumor 100% irradiated in ASMase WT and KO mice (Fig. 1A), indicating that the ASMase is not involved in the tumor control after a 100% RT tumor volume exposure. These results also suggest that the ASMase expression is essential in the host cells.

**Fig. 1.** ASMase is essential for the PVRT-induced tumor response. (A) ASMase KO and WT mice bearing subcutaneous LLC tumors were irradiated with 15Gy on either PVRT or all (100%) of the tumor area. Experiment was done 5 times, with a total of 7-10 mice per group (ASMase WT: NoRT n= 7; 50% n= 9; 100% n= 8 and ASMase KO: NoRT n= 7; 50% n= 10; 100% n= 9). Data have been normalized and pooled to show a unique graph with both males and females. (B) Graph of the tumor growth delay experiment described above for the ASMase WT mice. (C) Graph of the tumor growth delay experiment described above for the ASMase KO mice. Statistical analysis: Ordinary one-way ANOVA on the last tumor measurements for each group with post hoc Tukey's Multiple comparisons tests: ns=non-significant, \* p-value < 0.05.



*Pharmacological inhibition of ceramide-enriched lipid raft formation disrupts the PVRT-induced immune tumor response*

To further confirm the role of ASMase and ceramide in PVRT response, we used a biochemical approach in addition to the genetic approach used in the previous experiment described above. When activated, ASMase hydrolyses sphingomyelin and generates ceramide which initiates the assembly of cholesterol-and ceramide-rich lipid rafts (CRMs) [29, 30]. It has been previously demonstrated that methyl cyclodextrin (MCD) depletes membrane cholesterol notably from ceramide/cholesterol monolayer and thus disrupts the CRMs [31]. When LLC-tumor bearing C<sub>57</sub>Bl/6 mice were treated with MCD, while there was no effect on the tumor growth of the non-irradiated tumors (no significant difference between No RT control and treated groups), the sensitivity to PVRT was abolished (Fig. 2A and Fig. 2C). This suggests that CRM generation is essential for the tumor response to PVRT.

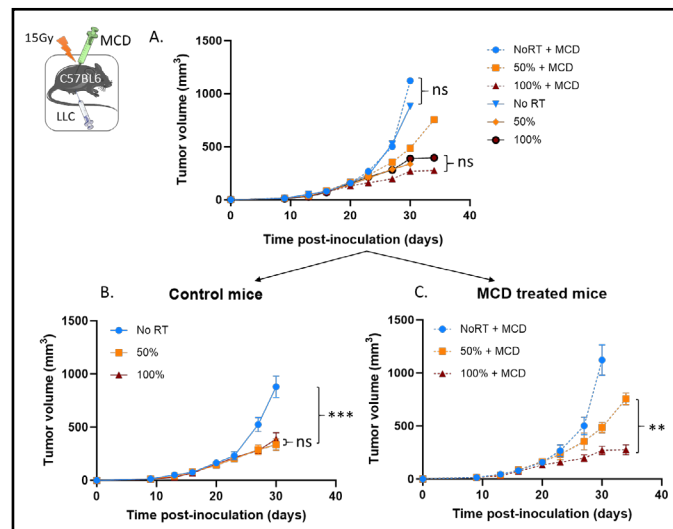


**Fig. 2.** Pharmacological ASMase inhibition disrupts the PVRT-induced tumor response. (A) C57BL6 mice bearing subcutaneous LLC tumors were irradiated with 15Gy on either PVRT or all (100%) of the tumor area. Mice are treated with water (control group) or Methyl-cyclodextrin (100mg/kg, 2h pre-RT & once a week, IP) (MCD group). Experiment was done 2 times, with 5 mice per group. Data have been normalized and pooled to show a unique graph with both males and females. (B) Graph of the tumor growth delay experiment described above for the control mice. (C) Graph of the tumor growth delay experiment described above for the MCD-treated mice. Statistical analysis: Ordinary one-way ANOVA on the last tumor measurements for each group with post hoc Tukey's Multiple comparisons tests: ns=non-significant, \*\* p-value < 0.01, \*\*\* p-value < 0.001.

*ASMase is essential for RT-induced ICAM-1 expression*

As PVRT has previously been shown to activate ICAM-1 expression [13, 14], we tested the effect of PVRT and 100% irradiation on ICAM-1 expression in ASMase-depleted and wild-type mice. Expression was detected by IHC in tumors collected 24 hours after exposure (Fig. 3A).

While the baseline ICAM-1 expression (No RT) is similar in ASMase WT and KO mice (p-value=0.72), their response to radiation is different (Fig. 3B and C). As expected, we observed increased expression of ICAM-1 in wild-type mice, in both the fully irradiated (100%) (average expression of 41%) and PVRT tumors compared to the non-irradiated controls (30.8%). The PVRT tumors from wild-type mice showed enhanced ICAM-1 expression in both the irradiated (In Field = IF) (42.5%) and unirradiated (Off Field = OF) (42.8%) fields. However, increased ICAM-1 was not observed in any of the irradiated tumors growing in ASMase KO mice (average no RT: 36.2% OF: 37.6%, IF: 38.8%, 100%: 33.1%). ICAM-1/IHC was quantified as the percent of ICAM-stained cells (Fig 3B and C), revealing that these differences were statistically significant at the 5% significance level. In addition, we compared the ICAM-1 relative expression (normalized from the No RT mean) of the WT and KO mice. We observed a significant decreased ICAM-1 expression in the ASMase KO mice compared to the WT in the 50% OF, the 50% IF, and the 100%-irradiated tumors (Fig. 3D). Altogether, these data demonstrate that ASMase is necessary for the ICAM-1 expression induced by both PVRT and 100% RT in the LLC model.

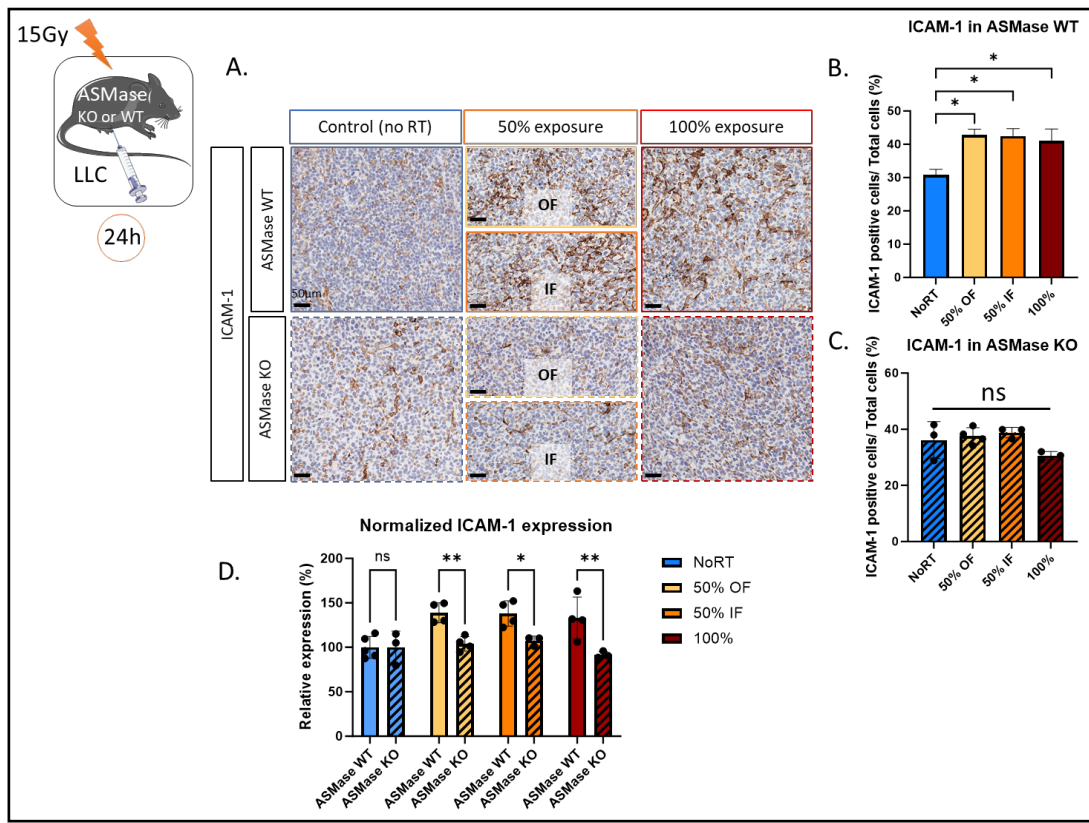


**Fig. 3.** ASmase is necessary for the ICAM-1 expression induced by RT in the LLC cancer model. (A) Representative ICAM-1-stained images (AF796) with Hematoxylin counterstained nuclei for the unirradiated controls, in-field (IF) hemi-irradiated tumors, Off-field (OF) hemi-irradiated tumors (Half of the tumor not receiving the radiation), and the fully (100% volume) irradiated tumors of ASmase WT and KO mice. Mice are sacrificed 24 hours after the radiation therapy. Staining performed by the molecular cytology core facility in MSKCC. (B) Quantification of the ICAM-1-positive cells/Total cell number from a representative experiment with 4-5 ASmase WT mice per treatment group (NoRT n= 4 mice; 50% OF n= 4; 50% IF n= 4; 100% n=4). (C) Quantification of the ICAM-1-positive cells/Total cell number from a representative experiment with 3-4 ASmase KO mice per treatment group (NoRT n= 3 mice; 50% OF n= 4; 50% IF n= 4; 100% n=3). (D) Comparison of the relative expression of ICAM-1 (normalized from NoRT mean expression) in ASmase WT and KO mice. Statistical analysis: Ordinary one-way ANOVA with post hoc Tukey's Multiple comparisons tests, on the area of the positive signal compared to the total area for each group: \* p-value < 0.05, \*\* p-value < 0.01.

#### *ASmase is essential for radiation induced CD8<sup>+</sup> T cell infiltration*

It has been previously shown that PVRT can stimulate CD8<sup>+</sup> T cell tumor infiltration and this effect can be abolished by neutralizing ICAM-1 antibody treatment [13, 14]. We therefore stained LLC tumors for the presence of CD8<sup>+</sup> T cells (Fig. 4A). There was no significant difference (p-value=0.48) between the baseline (No RT) of CD8<sup>+</sup> T cells expression in WT and KO mice. In the ASmase WT mice, we replicated our previously published data by showing an increased CD8<sup>+</sup> T cell infiltration following PVRT, both in the irradiated and unirradiated volumes parts of the tumor compared to the No RT group. Similar levels of infiltration were observed in the 100% RT group, but this failed to reach significance (p-value=0.17) (average no RT: 2.6% OF: 6.4%, IF: 6.2%, 100%: 5.3%) (Fig. 4B). However, in the ASmase KO mice, no significant increase in CD8<sup>+</sup> T cells was observed (average No RT: 4.6% OF: 4.4%, IF: 3.9%, 100%: 2.9%) (Fig. 4C). By comparing the relative percentage of CD8-positive cells in both ASmase WT and KO mice, we showed a significant loss of CD8<sup>+</sup> T cells infiltration

in the ASMase-depleted mice in both PVRT groups and in the 100% RT (Fig. 4D). These results show the key role of the ASMase in the CD8<sup>+</sup> T cells-mediated PVRT-induced immune response, and to a lesser extent in tumors fully exposed to RT.

*ASMase is essential for STING activation following PVRT*

It has previously been demonstrated that PVRT activates STING in the LLC cancer model [14]. To extend these findings, IHC was used to assess STING expression in ASMase WT and KO mice following PVRT or 100% exposure (Fig. 5A). In ASMase WT mice, PVRT induces an increased expression of STING in both IF and OF parts of the PVRT tumors compared to the non-irradiated ones. There is no significant increased expression of STING (p-value=0.17) in tumors that have received 100% exposure RT (average No RT: 17.6% OF: 30.2%, IF: 26.3%, 100%: 25.6%) (Fig. 5B). When the same experiment was performed in ASMase KO mice, the increased expression of STING following PVRT is lost. There are no differences between all the groups (average No RT: 20.2% OF: 18.7%, IF: 21.1%, 100%: 20.2%) (Fig. 5C). Similarly, there is no significant difference (p-value=0.66) between the baseline (NoRT) STING expression in WT and KO mice. The comparison of the STING relative expression between ASMase WT and KO mice showed a significantly higher expression of STING in the WT mice in both PVRT groups. This difference is not found in the 100% groups (Fig. 5D). These data bring to light the essential role of ASMase in the PVRT-induced activation of STING.

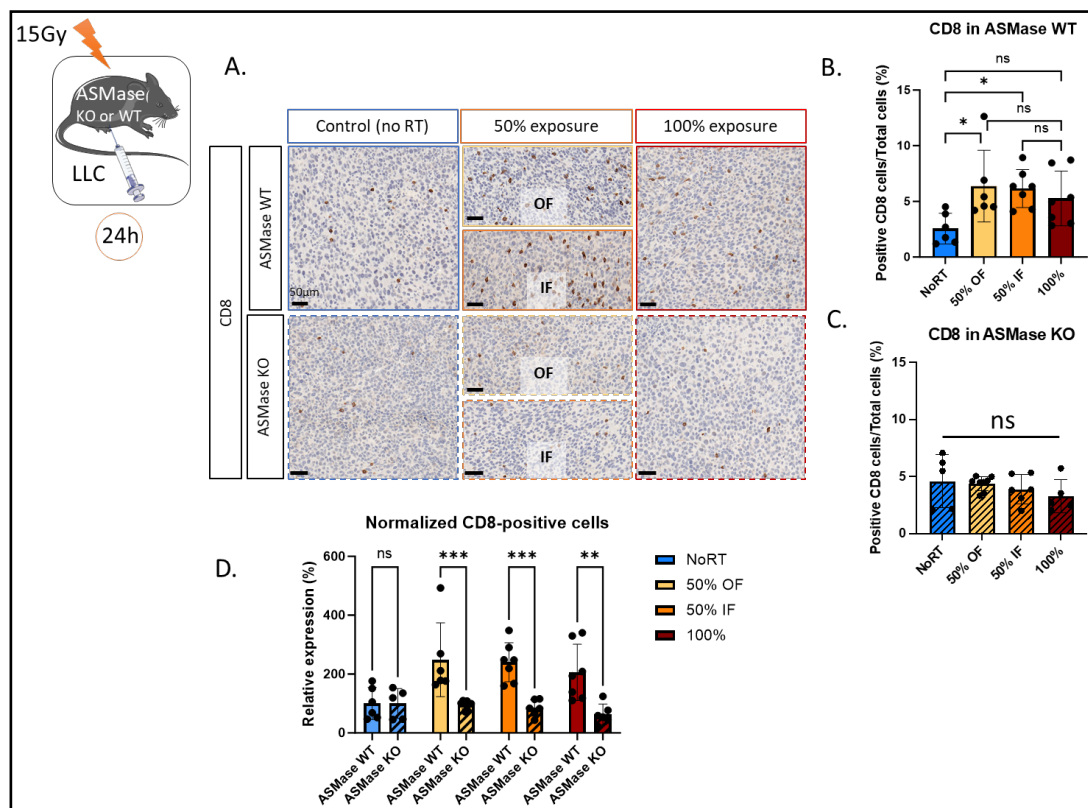


**Fig. 4.** ASMase is necessary for the CD8<sup>+</sup> T cell infiltration induced by PVRT. (A) Representative CD8-stained images with Hematoxylin counterstained nuclei for the unirradiated controls, in-field (IF) hemi-irradiated tumors, Off-field (OF) hemi-irradiated tumors (Half of the tumor not receiving the radiation), and the fully (100% volume) irradiated tumors of ASMase WT and KO mice. Mice are sacrificed 24 hours after the radiation therapy. Staining performed by the molecular cytology core facility in MSKCC. (B) Quantification of the CD8-positive cells/Total cell number from a representative experiment with 6-7 ASMase WT mice per treatment group (NoRT n= 6 mice; 50% OF n= 6; 50% IF n= 7; 100% n=7). (C) Quantification of the CD8-positive cells/Total cell number from a representative experiment with 5-8 ASMase KO mice per treatment group (NoRT n= 5 mice; 50% OF n= 8; 50% IF n= 6; 100% n=5). (D) Comparison of the relative expression of CD8 (normalized from NoRT mean expression) in ASMase WT and KO mice. Statistical analysis: Ordinary one-way ANOVA with post hoc Tukey's Multiple comparisons tests, on the area of the positive signal compared to the total area for each group: \* p-value < 0.05, \*\* p-value < 0.01, \*\*\* p-value < 0.001.

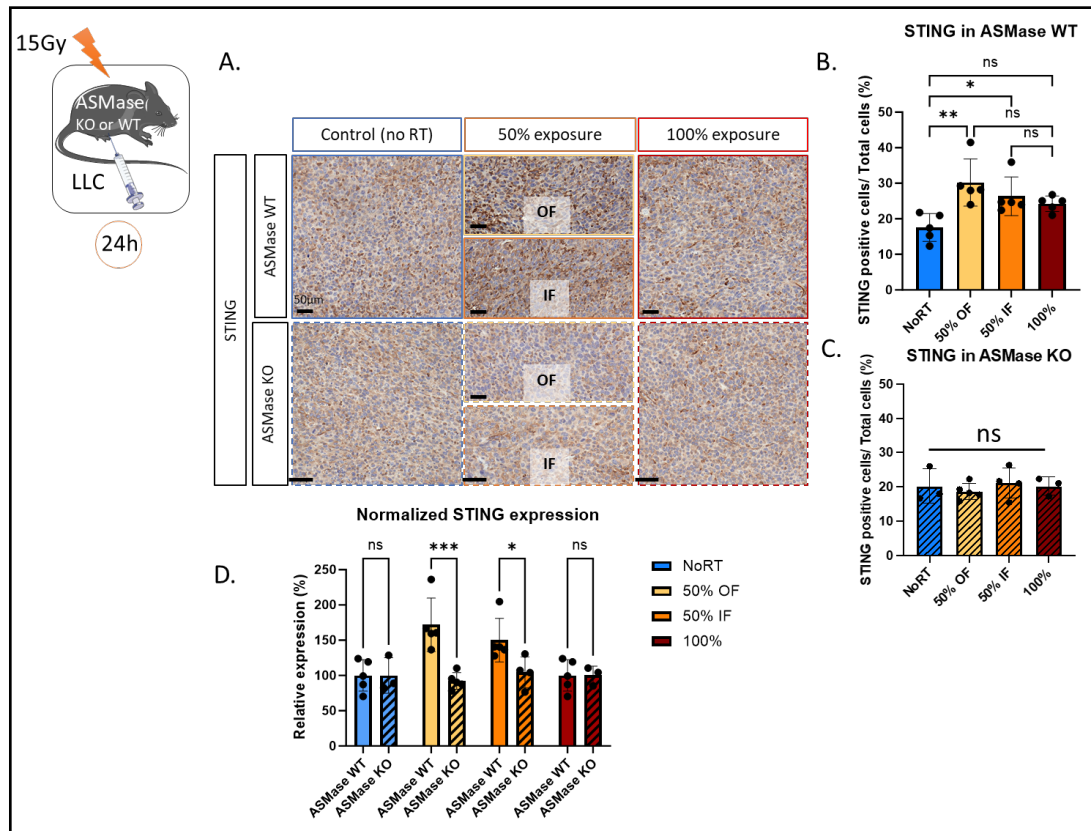


**Fig. 5.** ASMAse is necessary for the STING-expression induced by PVRT. (A) Representative STING-stained images with Hematoxylin counterstained nuclei for the unirradiated controls, in-field (IF) hemi-irradiated tumors, Off-field (OF) hemi-irradiated tumors (Half of the tumor not receiving the radiation), and the fully (100% volume) irradiated tumors of ASMAse WT and KO mice. Mice are sacrificed 24 hours after the radiation therapy. Staining performed by the molecular cytology core facility in MSKCC. (B) Quantification of the STING-positive cells/Total cell number from a representative experiment with 5 ASMAse WT mice per treatment group. (C) Quantification of the STING-positive cells/Total cell number from a representative experiment with 3-5 ASMAse KO mice per treatment group (NoRT n= 3 mice; 50% OF n= 5; 50% IF n= 4; 100% n=3). (D) Comparison of the relative expression of STING (normalized from NoRT mean expression) in ASMAse WT and KO mice. Statistical analysis: Ordinary one-way ANOVA with post hoc Tukey's Multiple comparisons tests, on the area of the positive signal compared to the total area for each group: \* p-value < 0.05, \*\* p-value < 0.01, \*\*\* p-value < 0.001.

### *The PVRT-induced immune tumor response does not involve polymorphonuclear neutrophils*

Polymorphonuclear neutrophils (PMNs) are the most abundant innate immune cells in the body. Animal and human studies provide solid experimental evidence that PMNs can be cancer-killing effector cells and may potentially be sufficient to destroy tumors [32]. PMNs have been reported to bind to ICAM-1 on the inflamed endothelial cells [33]. Therefore, we investigated the role of PMNs in the PVRT-induced tumor response. C57Bl/6 mice with LLC tumors were pre-treated with anti-IgG2 $\alpha$  antibody for the control group, or anti-Ly6G to deplete the PMNs (Supp Fig. 2), 24 hours before RT (Fig. 6A). Control mice treated with the anti-IgG2 $\alpha$  show the same tumor response following PVRT and 100% RT (Fig. 6B). Similarly, mice depleted of PMNs due to the anti-Ly6G treatment, have the same tumor response following PVRT and 100% RT (Fig. 6C). Similarly, there is no significant difference in the tumor response following No RT, PVRT (50%), and 100% RT between the control and the PMN-depleted mice (Fig. 6A). These data indicate that the PMNs were not involved in the PVRT-induced immune tumor response.

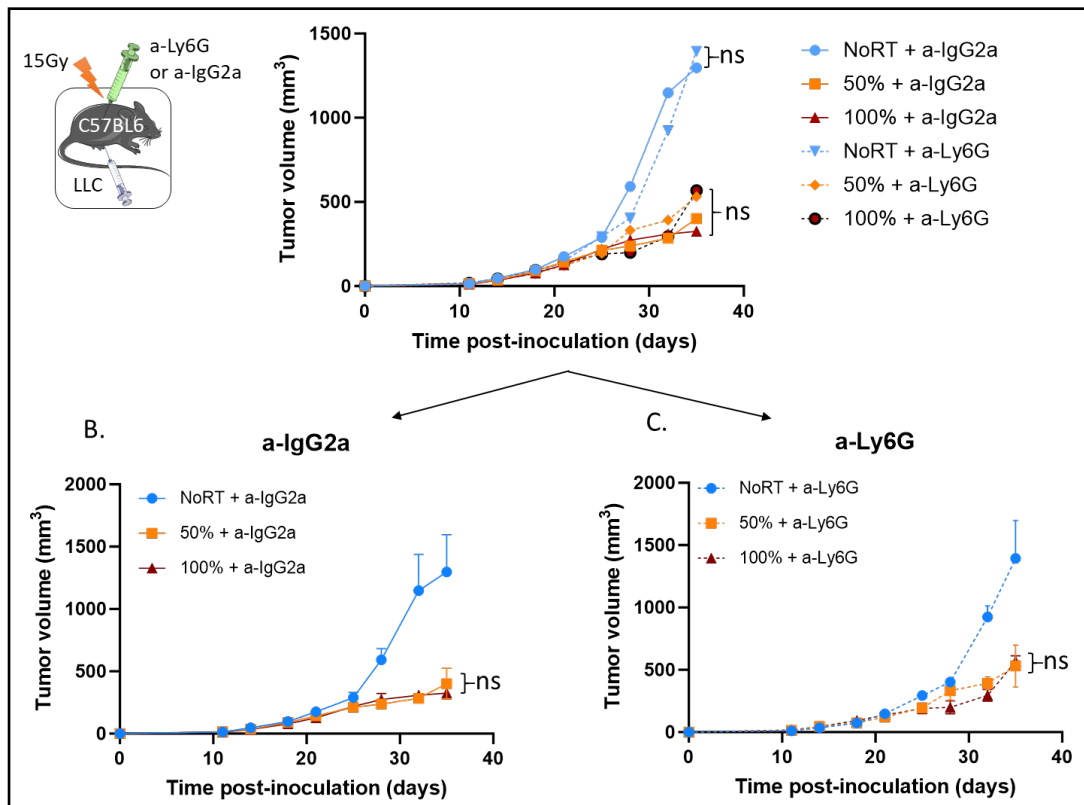


**Fig. 6.** Polymorphonuclear neutrophil depletion has no effect on the PVRT-induced tumor response. (A) C57BL/6 mice bearing subcutaneous LLC tumors were irradiated with 15Gy on either PVRT or all (100%) of the tumor area. Mice are treated with an IgG2a antibody (control group) or Ly6G antibody (PMN-depleted group) (200 $\mu$ g/mouse, 24h pre-RT & twice a week, IP). Experiment was done 2 times, with 5 mice per group. Data have been normalized and pooled to show a unique graph with both males and females. (B) Graph of the tumor growth delay experiment described above for the control mice (a-IgG2 $\alpha$  treated). (C) Graph of the tumor growth delay experiment described above for the PMN-depleted mice (a-Ly6G treated). Statistical analysis: Ordinary one-way ANOVA with post hoc Tukey's Multiple comparisons tests, on the last tumor measurements for each group: ns=non-significant

## Discussion

Our study investigates the biological changes induced by partial-volume radiation therapy (PVRT) in murine LLC tumors, focusing on the role of acid sphingomyelinase (ASMase) and the subsequent ceramide production, CRMs generation in mediating these effects.

While PVRT-induced tumor response has previously been studied, notably by our lab [13, 14], to our knowledge, it's the first time a study showed and described the involvement of the ceramide-producing by ASMase and CRMs generation in this tumor response. We also brought to light an unknown link between ASMase-ceramide, CRMS and STING activation. Indeed, we demonstrated that ASMase is essential for the STING pathway activation following PVRT, which is associated with increased infiltration of CD8<sup>+</sup> T cells and elevated intercellular adhesion molecule 1 (ICAM-1) expression in tumors. This response is markedly diminished in ASMase knockout (KO) mice, indicating the indispensability of ASMase in these processes. In addition, we have shown that the PMNs do not play a significant role in the PVRT-induced immune response.

This paper is consistent with previously published data showing that the PVRT-induced immune response allows a similar tumor control in the hemi-irradiated tumors than in the fully irradiated ones [13, 14]. Using pharmacological and genetic approaches, the study highlighted the central role of CRMs, generated through ASMase activation, and disrupted using Methyl Cyclodextrin (MCD) [34], in PVRT-induced anti-tumor immunity. This aligns with prior research identifying ceramide as a key mediator in radiation-induced vascular damage and immune activation [23, 26]. This study also suggests that the ceramide production by the activated ASMase, triggers the subsequent STING activation, ICAM-1 expression, and CD8+ T cell infiltration which are part of the immune activation pathway in response to PVRT previously described in the literature [13, 14].

CD8+ T cell infiltration is crucial in the tumor microenvironment, impacting tumor growth and progression [19, 35]. Previous studies indicated ASMase and ceramide's roles in immune regulation, though no direct evidence linked ASMase to CD8+ T cell infiltration post-irradiation [36, 37]. This study reveals ASMase's pivotal role in facilitating CD8+ T cell infiltration, crucial for PVRT-induced immune response [13, 14]. In previously published data [13], we showed that mice treated with a CD8-depleting antibody were strongly losing the PVRT-induced tumor response. Our paper corroborates those data.

Polymorphonuclear Neutrophils (PMNs) are the most abundant circulating immune cells and represent the first line of immune defense. However, the dynamic interplay between irradiation and neutrophils is a complex process that impacts radiation-based treatments [37, 38]. Intriguingly, our results revealed no discernible difference in tumor response following PVRT and 100% RT in both control and PMNs-depleted ones. These observations indicate that PMNs, despite their potency as effector cells after irradiation [38], do not appear to play a significant role in the PVRT-induced accelerated immune response at least in these tumor models tested here. However, there is a broader immune landscape in the tumor microenvironment [39] to explore. For example, the NK cells could be involved in the PVRT response. Indeed, their activity is modulated in response to certain types of RT [40]. Those cells will be part of future investigations. In addition, we are currently characterizing other immune cell populations, such as T cell resident memory (Trm) described recently [41].

Intercellular adhesion molecule-1 (ICAM-1) is essential in inflammatory reactions [42], providing crucial signals for T-cell activation [43] and the programming of memory CD8+ T cells [44]. ICAM-1 expression is triggered by inflammatory stimuli, including irradiation. Previous research showed that PVRT activates ICAM-1 expression [13, 14], which this study explored further in ASMase-depleted mice. In ASMase WT mice, ICAM-1 expression increased in fully irradiated tumors and PVRT-treated tumors, both in non-irradiated and irradiated regions. However, ASMase KO mice showed no significant variation in ICAM-1 expression across treatment groups, indicating ASMase's crucial role in ICAM-1 induction in response to PVRT. Sphingomyelinase and ceramide modulate lipid rafts [45], which are dynamic platforms for various cellular processes. MCD treatment disrupts ICAM-1 from these rafts, reducing cell adhesion [46]. These findings highlight the interplay between ASMase and adhesion molecules, offering insights into PVRT-induced immune responses.

Tumors are known to be more radioresistant when growing in ASMase KO mice than in wild-type: this was attributed to vascular apoptosis, rather than immune effects, which were also examined [23]. Our data shows that 100% irradiated tumors differ in their short-term response to radiation when grown in ASMase wild-type or knockout hosts, particularly for ICAM-1 expression. As the dose used (15Gy) was curative in both models: with complete tumor control achieved in the more radioresistant ASMase KO model, it would not be possible to measure increased sensitivity in the wild types.

Another question concerns how partial and total tumor irradiation are related. One possibility is that the underlying biology is identical: radiation stimulates an immune response capable of tumor control, regardless of radiation cell kill. The partial volume treatment serves only to make this apparent because tumor control cannot be attributed to a direct radiation effect. Indeed, it is known that radiation therapy promotes the release of tumor neoantigens during cancer cell death in addition to stimulating immune adjuvant

effects, engaging both innate and adaptive arms of the immune system and functioning like an in-situ vaccine, generating tumor-specific T cells with local as well as potentially distant, systemic effects [47]. Alternatively, the biology of 100% and PVRT-treated tumors may be different, for example, if tumor-resident cells are contributing to orchestrating the immune response, and the hemi-irradiation spares a portion of this hypothetical population. Indeed, immune cells, such as lymphocytes are among the most radiosensitive cells [48]. PVRT, by preserving a part of the tumor, its blood vessels, and the healthy tissues surrounding it, could overcome this problem and lead to an immune tumor response.

Partial-volume irradiation techniques have emerged as promising approaches to selectively irradiating smaller volumes within the tumor [10, 11] while sparing surrounding healthy tissues and organs adjacent to the tumor. Beyond their direct effects on tumor cells with reduced toxicity on healthy tissues, partial-volume irradiation methods have been found to elicit intriguing systemic responses known as the bystander and abscopal effects. Despite the promising potential of partial-volume irradiation approach in clinical human trials [10, 49] and their link to bystander and abscopal effects [1, 12] through immune system activation, the precise mechanisms underlying these effects are not yet fully understood. A more comprehensive understanding of the cellular and molecular processes involved is crucial for optimizing treatment strategies and harnessing these effects consistently, providing a potential avenue for enhanced therapeutic outcomes using this approach. We have previously demonstrated our ability to hemi-irradiated murine tumors and reliably recover the treated and untreated volumes for histology [13, 14]. However, because of technical limitations, we are not able to target conclusively less than 50% of the tumor, yet. It could be very interesting to determine the smallest irradiated area volume within a tumor target to get the best activation of the host's immune system. Similarly, we would like to be as close to the clinic as possible by delivering PVRT to the tumor as GRID/Lattice RT by alternating high-dose and low-dose areas as peaks and valleys.

Radiation-induced micronuclei and dsDNA are critical for anti-tumor immunity via cGAS sensing and STING activation [50]. A previous study showed that PVRT activates STING in the LLC cancer model [14]. In ASMase WT mice, STING expression increased in both irradiated and non-irradiated tumor parts following PVRT, but not after 100% RT, indicating different mechanisms for tumor volume control. In ASMase KO mice, the expected STING upregulation post-PVRT was absent, highlighting ASMase's crucial role in STING activation. Research showed that administration of Ceramide-C6 disrupts lipid rafts at the Golgi, hindering STING-dependent phosphorylation of TBK1 and IRF3 [19]. STING clustering in lipid rafts at the trans-Golgi network is essential for TBK1 and IRF3 recruitment, differing from STING clustering at the ER [51]. In addition, STING activation varies by tumor type, occurring via cGAS/STING or non-canonical ATM-driven pathways [14]. While our findings confirm the instrumental role of ASMase/ceramide in STING pathway activation following PVRT, several critical questions remain unanswered. Further studies on ASMase/ceramide regulation of TBK1 recruitment to STING, STING's post-Golgi trafficking, and their impact on CD8+ T cell infiltration and ICAM-1 expression.

This study highlights the significance of ASMase/ceramide function in PVRT-induced accelerated adoptive immune responses, paving the way for further investigations into novel therapeutic strategies that harness these effects to improve cancer treatment outcomes in tumors considered radiation resistant, that are still quite a challenge for this therapy. By comprehensively understanding the mechanisms involved, we may be able to optimize PVRT approaches and enhance their efficacy for metastatic lesions, ultimately contributing to more effective and targeted cancer therapies in the future.

In the study presented here, we recapitulated our previous finding, that hemi-volume irradiation of the tumor was sufficient for tumor control in the relatively radio-resistant LLC model. Using a genetic approach, we demonstrated that this is an ASMase-ceramide-dependent process. Likewise, we demonstrated that increased levels of CD8+ T cells, elevated ICAM-1 expression, and STING activation in tumors, are ASMase-ceramide dependent. Further, pharmacological inhibition of ASMase significantly reduced the tumor

response to hemi-irradiation, though inhibition of PMN cell infiltration was ineffective. Acid sphingomyelinase-derived ceramide is required to mediate a partial-volume radiation therapy-induced anti-tumor immune response which might show to be significant in the metastatic setting of this disease.

## Acknowledgements

We thank Ning Fan and others at the Molecular cytology core facility for their invaluable help (MSKCC). This work was supported by NIH grant P30 CA008748 (to SP).

The experiments and planning of the experimental work were done by Mickael Mathieu and Prerna R. Nepali. James Russell and John Humm helped us with PVRT planning and execution. AH-F oversaw the design of these experiments and overseeing the experimental work and analysis of the data. MM, PR, AH-F, JOD, JH helped with analyses of the results. Hadi Askarifirouzjaei and Melis Baltaci helped with the writing of the discussion.

This study was supported by research and development funds from the Departments of Radiation Oncology and Medical Physics, by National Cancer Institute Core Center grant P30 CA008748, and by a shared resources grant from the Memorial Sloan Kettering Cancer Center.

Geoffrey Beene Cancer Research Center for the purchase of the X-RAD 225Cx Microirradiator (Principal Investigator: J.O.D.).

## Statement of Ethics

All animal experiments were performed according to the ethical guidelines, following a protocol approved by the Institutional Animal Care and Use Committee (IACUC) at Memorial Sloan Kettering Cancer Center. Animals were housed at the Research Animal Resource Center (RARC) of Memorial Sloan Kettering Cancer Center. The facility is approved by the American Association for Accreditation of Laboratory Animal Care and is maintained following the regulations and standards of the United States Department of Agriculture and the Department of Health and Human Services, National Institutes of Health.

## Disclosure Statement

The authors have no conflicts of interest to declare.

## References

- 1 Kanagavelu S, Gupta S, Wu X, Philip S, Wattenberg MM, Hodge JW, Couto MD, Chung KD, Ahmed MM: *In vivo* effects of lattice radiation therapy on local and distant lung cancer: potential role of immunomodulation. *Radiat Res* 2014;182:149-162.
- 2 Kim W, Lee S, Seo D, Kim D, Kim K, Kim E, Kang J, Seong KM, Youn H, Youn B: Cellular Stress Responses in Radiotherapy. *Cells* 2019;8
- 3 Shao C, Folkard M, Michael BD, Prise KM: Targeted cytoplasmic irradiation induces bystander responses. *Proc Natl Acad Sci U S A* 2004;101:13495-13500.
- 4 Pilonis KA, Vanpouille-Box C, Demaria S: Combination of radiotherapy and immune checkpoint inhibitors. *Semin Radiat Oncol* 2015;25:28-33.
- 5 Lugade AA, Sorensen EW, Gerber SA, Moran JP, Frelinger JG, Lord EM: Radiation-induced IFN-gamma production within the tumor microenvironment influences antitumor immunity. *J Immunol* 2008;180:3132-3139.
- 6 Tesniere A, Panaretakis T, Kepp O, Apetoh L, Ghiringhelli F, Zitvogel L, Kroemer G: Molecular characteristics of immunogenic cancer cell death. *Cell Death Differ* 2008;15:3-12.
- 7 Siva S, MacManus MP, Martin RF, Martin OA: Abscopal effects of radiation therapy: a clinical review for the radiobiologist. *Cancer Lett* 2015;356:82-90.

- 8 Abuodeh Y, Venkat P, Kim S: Systematic review of case reports on the abscopal effect. *Curr Probl Cancer* 2016;40:25-37.
- 9 Postow MA, Callahan MK, Barker CA, Yamada Y, Yuan J, Kitano S, Mu Z, Rasalan T, Adamow M, Ritter E, Sedrak C, Jungbluth AA, Chua R, Yang AS, Roman RA, Rosner S, Benson B, Allison JP, Lesokhin AM, Gnjatic S, Wolchok JD: Immunologic correlates of the abscopal effect in a patient with melanoma. *N Engl J Med* 2012;366:925-931.
- 10 Duriseti S, Kavanaugh J, Goddu S, Price A, Knutson N, Reynoso F, Michalski J, Mutic S, Robinson C, Spraker MB: Spatially fractionated stereotactic body radiation therapy (Lattice) for large tumors. *Adv Radiat Oncol* 2021;6:100639.
- 11 Amendola BE, Perez NC, Amendola MA, Wu X: The Use of Lattice Radiation Therapy in Patients With Voluminous Tumors. *International Journal of Radiation Oncology, Biology, Physics* 2020;108:e520.
- 12 Peters ME, Shareef MM, Gupta S, Zagurovskaya-Sultanov M, Kadhim M, Mohiuddin M, Ahmed MM: Potential utilization of bystander/abscopal-mediated signal transduction events in the treatment of solid tumors. *Current Signal Transduction Therapy* 2007;2:129-143.
- 13 Markovsky E, Budhu S, Samstein RM, Li H, Russell J, Zhang Z, Drill E, Bodden C, Chen Q, Powell SN, Merghoub T, Wolchok JD, Humm J, Deasy JO, Haimovitz-Friedman A: An Antitumor Immune Response Is Evoked by Partial-Volume Single-Dose Radiation in 2 Murine Models. *Int J Radiat Oncol Biol Phys* 2019;103:697-708.
- 14 Mathieu M, Budhu S, Nepali PR, Russell J, Powell SN, Humm J, Deasy JO, Haimovitz-Friedman A: Activation of Sting in Response to Partial-Tumor Radiation Exposure. *Int J Radiat Oncol Biol Phys* 2023
- 15 Sun L, Wu J, Du F, Chen X, Chen ZJ: Cyclic GMP-AMP synthase is a cytosolic DNA sensor that activates the type I interferon pathway. *Science* 2013;339:786-791.
- 16 Ergun SL, Fernandez D, Weiss TM, Li L: STING Polymer Structure Reveals Mechanisms for Activation, Hyperactivation, and Inhibition. *Cell* 2019;178:290-301 e210.
- 17 Zhang C, Shang G, Gui X, Zhang X, Bai XC, Chen ZJ: Structural basis of STING binding with and phosphorylation by TBK1. *Nature* 2019;567:394-398.
- 18 Dobbs N, Burnaevskiy N, Chen D, Gonugunta VK, Alto NM, Yan N: STING Activation by Translocation from the ER Is Associated with Infection and Autoinflammatory Disease. *Cell Host Microbe* 2015;18:157-168.
- 19 Mukai K, Konno H, Akiba T, Uemura T, Waguri S, Kobayashi T, Barber GN, Arai H, Taguchi T: Activation of STING requires palmitoylation at the Golgi. *Nat Commun* 2016;7:11932.
- 20 Barber GN: STING: infection, inflammation and cancer. *Nat Rev Immunol* 2015;15:760-770.
- 21 Ablasser A, Schmid-Burgk JL, Hemmerling I, Horvath GL, Schmidt T, Latz E, Hornung V: Cell intrinsic immunity spreads to bystander cells via the intercellular transfer of cGAMP. *Nature* 2013;503:530-534.
- 22 Ablasser A, Chen ZJ: cGAS in action: Expanding roles in immunity and inflammation. *Science* 2019;363
- 23 Garcia-Barros M, Paris F, Cordon-Cardo C, Lyden D, Rafii S, Haimovitz-Friedman A, Fuks Z, Kolesnick R: Tumor response to radiotherapy regulated by endothelial cell apoptosis. *Science* 2003;300:1155-1159.
- 24 Sharma D, Czarnota GJ: Role of acid sphingomyelinase-induced ceramide generation in response to radiation. *Oncotarget* 2019;10:6-7.
- 25 Paris F, Fuks Z, Capodici P, Juan G, Ehleiter D, Schwartz JL, Seddon AP, Cordon-Cardo C, Haimovitz-Friedman A: Endothelial apoptosis as the primary lesion initiating intestinal radiation damage in mice. *Science* 2001;293:293-297.
- 26 Haimovitz-Friedman A, Kan CC, Ehleiter D, Persaud RS, McLoughlin M, Fuks Z, Kolesnick RN: Ionizing radiation acts on cellular membranes to generate ceramide and initiate apoptosis. *J Exp Med* 1994;180:525-535.
- 27 Deng X, Yin X, Allan R, Lu DD, Maurer CW, Haimovitz-Friedman A, Fuks Z, Shaham S, Kolesnick R: Ceramide biogenesis is required for radiation-induced apoptosis in the germ line of *C. elegans*. *Science* 2008;322:110-115.
- 28 Jeong J, Chen Q, Febo R, Yang J, Pham H, Xiong JP, Zanzonico PB, Deasy JO, Humm JL, Mageras GS: Adaptation, Commissioning, and Evaluation of a 3D Treatment Planning System for High-Resolution Small-Animal Irradiation. *Technol Cancer Res Treat* 2016;15:460-471.
- 29 Ira, Zou S, Ramirez DM, Vanderlip S, Ogilvie W, Jakubek ZJ, Johnston LJ: Enzymatic generation of ceramide induces membrane restructuring: Correlated AFM and fluorescence imaging of supported bilayers. *J Struct Biol* 2009;168:78-89.
- 30 Johnston I, Johnston LJ: Ceramide promotes restructuring of model raft membranes. *Langmuir* 2006;22:11284-11289.

- 31 Mandal P, Noutsi P, Chaieb S: Cholesterol Depletion from a Ceramide/Cholesterol Mixed Monolayer: A Brewster Angle Microscope Study. *Sci Rep* 2016;6:26907.
- 32 Nathan C: Neutrophils and immunity: challenges and opportunities. *Nat Rev Immunol* 2006;6:173-182.
- 33 Yang L, Froio RM, Sciuto TE, Dvorak AM, Alon R, Lusciuskas FW: ICAM-1 regulates neutrophil adhesion and transcellular migration of TNF-alpha-activated vascular endothelium under flow. *Blood* 2005;106:584-592.
- 34 Cremesti A, Paris F, Grassme H, Holler N, Tschopp J, Fuks Z, Gulbins E, Kolesnick R: Ceramide enables fas to cap and kill. *J Biol Chem* 2001;276:23954-23961.
- 35 Peske JD, Woods AB, Engelhard VH: Control of CD8 T-Cell Infiltration into Tumors by Vasculature and Microenvironment. *Adv Cancer Res* 2015;128:263-307.
- 36 Hose M, Gunther A, Naser E, Schumacher F, Schonberger T, Falkenstein J, Papadamakis A, Kleuser B, Becker KA, Gulbins E, Haimovitz-Friedman A, Buer J, Westendorf AM, Hansen W: Cell-intrinsic ceramides determine T cell function during melanoma progression. *Elife* 2022;11
- 37 Hu J, Pan M, Wang Y, Zhu Y, Wang M: Functional plasticity of neutrophils after low- or high-dose irradiation in cancer treatment - A mini review. *Front Immunol* 2023;14:1169670.
- 38 Takeshima T, Pop LM, Laine A, Iyengar P, Vitetta ES, Hannan R: Key role for neutrophils in radiation-induced antitumor immune responses: Potentiation with G-CSF. *Proc Natl Acad Sci U S A* 2016;113:11300-11305.
- 39 Binnewies M, Roberts EW, Kersten K, Chan V, Fearon DF, Merad M, Coussens LM, Gaborilovich DI, Ostrand-Rosenberg S, Hedrick CC, Vonderheide RH, Pittet MJ, Jain RK, Zou W, Howcroft TK, Woodhouse EC, Weinberg RA, Krummel MF: Understanding the tumor immune microenvironment (TIME) for effective therapy. *Nat Med* 2018;24:541-550.
- 40 Chen J, Liu X, Zeng Z, Li J, Luo Y, Sun W, Gong Y, Zhang J, Wu Q, Xie C: Immunomodulation of NK Cells by Ionizing Radiation. *Front Oncol* 2020;10:874.
- 41 Arina A, Beckett M, Fernandez C, Zheng W, Pitroda S, Chmura SJ, Luke JJ, Forde M, Hou Y, Burnette B, Mauceri H, Lowy I, Sims T, Khodarev N, Fu Y-X, Weichselbaum RR: Tumor-reprogrammed resident T cells resist radiation to control tumors. *Nature Communications* 2019;10:3959.
- 42 Bui TM, Wiesolek HL, Sumagin R: ICAM-1: A master regulator of cellular responses in inflammation, injury resolution, and tumorigenesis. *J Leukoc Biol* 2020;108:787-799.
- 43 Chirathaworn C, Kohlmeier JE, Tibbetts SA, Rumsey LM, Chan MA, Benedict SH: Stimulation through intercellular adhesion molecule-1 provides a second signal for T cell activation. *J Immunol* 2002;168:5530-5537.
- 44 Cox MA, Barnum SR, Bullard DC, Zajac AJ: ICAM-1-dependent tuning of memory CD8 T-cell responses following acute infection. *Proc Natl Acad Sci U S A* 2013;110:1416-1421.
- 45 Cremesti AE, Goni FM, Kolesnick R: Role of sphingomyelinase and ceramide in modulating rafts: do biophysical properties determine biologic outcome? *FEBS Lett* 2002;531:47-53.
- 46 Zhang S, Liu T, Liang H, Zhang H, Yan D, Wang N, Jiang X, Feng W, Wang J, Li P, Li Z: Lipid rafts uncouple surface expression of transmembrane TNF-alpha from its cytotoxicity associated with ICAM-1 clustering in Raji cells. *Mol Immunol* 2009;46:1551-1560.
- 47 Kaminski JM, Shinohara E, Summers JB, Niermann KJ, Morimoto A, Brousal J: The controversial abscopal effect. *Cancer Treat Rev* 2005;31:159-172.
- 48 Nakamura N, Kusunoki Y, Akiyama M: Radiosensitivity of CD4 or CD8 positive human T-lymphocytes by an *in vitro* colony formation assay. *Radiat Res* 1990;123:224-227.
- 49 Korpics MC, Onderdonk BE, Dadey RE, Hara JH, Karapetyan L, Zha Y, Karrison TG, Olson AC, Fleming GF, Weichselbaum RR, Bao R, Chmura SJ, Luke JJ: Partial tumor irradiation plus pembrolizumab in treating large advanced solid tumor metastases. *J Clin Invest* 2023;133
- 50 Constanzo J, Faget J, Ursino C, Badie C, Pouget JP: Radiation-Induced Immunity and Toxicities: The Versatility of the cGAS-STING Pathway. *Front Immunol* 2021;12:680503.
- 51 Shang G, Zhang C, Chen ZJ, Bai XC, Zhang X: Cryo-EM structures of STING reveal its mechanism of activation by cyclic GMP-AMP. *Nature* 2019;567:389-393.